32. S. Valututti, S. Müller, M. Cella, E. Padovan, A. Lanzavecchia, *Nature* **375**, 148 (1995); A. Viola and A. Lanzavecchia. *Science* **273,** 104 (1996).
33. H. M. McConnell, T. H. Watts, R. M. Weis, A. A. Brian, *Biochim. Biophys. Acta* **864**, 95 (1986); E. Sackmann, *Science* **271**, 43 (1996).
34. D. A. Wettstein, J. J. Boniface, P. A. Reay, H. Schild, M. M. Davis, *J. Exp. Med.* **174**, 219 (1991).
35. K. K. Baldwin, P. A. Reay, L. Wu, A. Farr, M. M. Davis, *ibid.* **189**, 13 (1999).
36. W. F. Wade, J. H. Freed, M. Edidin, *J. Cell Biol.* **109**, 3325 (1989); W. F. Wade, E. D. Ward, E. F. Rosloniec, B. G. Barisas, J. H. Freed, *Int. Immunol.* **6**, 1457 (1994).
37. A. Y. Lin, *et al.*, *Science* **249**, 677 (1990).
38. D. Axelrod, D. E. Koppel, J. Schlessinger, E. L. Elson, W. W. Webb, *Biophys. J.* **16**, 1055 (1976).
39. M. L. Dustin *et al.*, *J. Biol. Chem.* **272**, 30889 (1997).
40. The density and number of accumulated molecules in different regions of the contact area were calculated as the accumulated density (molecules/μm^2) = {[intensity in masked area (fluorescence units/μm^2)] − [intensity in neighboring area (fluorescence units/μm^2)]} ÷ specific activity (fluorescence units/molecule).
41. Planar bilayers with E^k-GPI and ICAM-1–GPI at 200 molecules/μm^2 each were formed on 100-μm glass beads (Mo-Sci, Rolla, MO). Bilayers on large glass beads behave identically to planar bilayers. The E^k on the coated glass beads (25 mg per well) was loaded with peptides as above. Beads were combined with 10^5 rested T cells in 200 μl of RPMI-1640, 10% fetal bovine serum. [^{3}H]Thymidine (0.2 μCi) was added on day 3, the plates were incubated an additional 24 hours, and then the cells were harvested on filters for scintillation counting.
42. D. Gay, C. Coeshott, W. Golde, J. Kappler, P. Marrack, *J. Immunol.* **136**, 2026 (1986).
43. We thank R. Houdei for technical assistance and N. Desai for advice on imaging and data analysis; D. Donermeyer for generation of the 3.L2 TCR transgenic mouse lacking CD4; E. Unanue for inspiring our efforts; E. Elson for help with FPR and the loan of the argon ion laser; J. Heuser and H. Hiyakawa for single-particle imaging; A. Chan, G. Kersh, M. Thomas, E. Unanue, and H. Virgin for critical reading of the manuscript; and J. Smith for final preparation of the manuscript. Supported by grants from the Whitaker Foundation (M.L.D.), the Arthritis Foundation (M.L.D.), the Howard Hughes Medical Institute (M.M.D.), and the NIH (M.L.D., M.M.D., P.M.A, and A.S.S.).

15 March 1999; accepted 1 June 1999

Variations in Atmospheric N_2O Concentration During Abrupt Climatic Changes

J. Flückiger,[1] A. Dällenbach,[1] T. Blunier,[1]* B. Stauffer,[1]† T. F. Stocker,[1] D. Raynaud,[2] J.-M. Barnola[2]

Nitrous oxide (N_2O) is an important greenhouse gas that is presently increasing at a rate of 0.25 percent per year. Records measured along two ice cores from Summit in Central Greenland provide information about variations in atmospheric N_2O concentration in the past. The record covering the past millennium reduces the uncertainty regarding the preindustrial concentration. Records covering the last glacial-interglacial transition and a fast climatic change during the last ice age show that the N_2O concentration changed in parallel with fast temperature variations in the Northern Hemisphere. This provides important information about the response of the environment to global climatic changes.

Nitrous oxide (N_2O) is an atmospheric trace gas with a relatively long lifetime of about 120 years (*1*). The main sources of N_2O in preindustrial times have been tropical soils, the ocean in upwelling regions, and soils in temperate regions (estimated contributions are 45, 30, and 25%, respectively, but with high uncertainties) (*1*). The main sink is photodissociation in the stratosphere (*1*). The atmospheric concentration of this greenhouse gas [which, apart from water vapor, is third in importance after carbon dioxide (CO_2) and methane (CH_4)] reached 314 parts per billion by volume (ppbv) in 1998 (*2*) and increases by about 0.25% per year (*1*). Knowledge about the atmospheric N_2O concentration before 1976 comes mainly from ice core analyses (*3*–*7*). Our record covering the past millennium allows us to narrow the range of the preindustrial concentration.

Records of CH_4 variations parallel to climatic oscillations have provided a wealth of information about the global significance of climatic oscillations and about the response of the environment to such variations (*8*–*10*). Like CH_4, N_2O has an important source in the tropics [wet forest soils and dry savannahs for N_2O; wetlands for CH_4 (*1*)], but in contrast to CH_4 it has an important oceanic source too. Therefore, we expect that our measurements, which cover time periods of drastic climate changes, will provide new information about environmental responses to those changes. We present examples from the last glacial-interglacial transition [16.5 to 10.5 thousand years before the present (kyr BP)] and from a fast climate oscillation during the last ice age (37.0 to 32.5 kyr BP).

The air trapped in polar ice samples was extracted with the melt-refreezing method used for CH_4 analyses (*10*, *11*). The N_2O concentration of the extracted air was measured with a gas chromatograph equipped with an electron capture detector. Tests with bubble-free ice and standard gas (the working standard was 304 ± 4 ppbv) confirmed that N_2O can be extracted with the melt-refreezing method despite the high solubility of N_2O in water (*12*), if the freezing speed is kept low. The small sample size (about 40 g) allowed us to measure several samples per annual layer for samples from this millennium as well as one sample per annual layer for the transition from the last glacial epoch to the Holocene. Data presented in this study are not corrected for gravitational fractionation (*13*).

Samples for the first measurement series, covering the past 1000 years (Fig. 1), are from cores drilled at Summit (central Greenland, 72°34′N, 37°38′W) as part of the EUROCORE project and the Greenland Ice Core Project (GRIP). The preindustrial N_2O concentration was relatively stable, with an average of 270 ± 5 ppbv for the time period between 1400 and 1750 A.D. Previously published data (*3*–*6*) are highly scattered and allow only a rough estimate of the preindustrial concentration of between 260 and 285 ppbv (Fig. 1). An exception are the precise results by Machida *et al.* (*7*) covering the past 300 years. The low scatter of our measurements and the good agreement with the measurements by Machida *et al.*, which were performed with a dry extraction technique, as well as the good agreement with the direct measurements on atmospheric air (*14*) and firn air measurements from Antarctica (*15*), indicate that our measurements for this time period are reliable and allow us to investigate changes in the atmospheric N_2O concentration that occurred together with climatic changes in past climate epochs.

In Fig. 2, the N_2O record for the transition period from the last glacial epoch to the Holocene measured along the GRIP ice core is compared with the GRIP records of oxygen isotope $\delta^{18}O$ (*16*) (used as a proxy for temperature) and CH_4 (*8*, *17*). The N_2O concentration increased

[1]Climate and Environmental Physics, Physics Institute, University of Bern, Sidlerstrasse 5, CH-3012 Bern, Switzerland. [2]CNRS Laboratoire de Glaciologie et Géophysique de l'Environnement (LGGE), Boîte Postale 96, 38402 St Martin d'Hères Cedex, Grenoble, France.

*Present address: Princeton University, Princeton, NJ 08544, USA.

†To whom correspondence should be addressed. E-mail: stauffer@climate.unibe.ch

during the transition from around 200 ppbv in the late glacial epoch to about 270 ppbv in the early Holocene. This increase was interrupted by a decrease during the Younger Dryas (YD) period (12.7 to 11.6 kyr BP).

The N_2O record shows a few surprisingly high values, which deviate from their neighboring samples (partly from the same core section) by much more than our mean analytical reproducibility (3.7 ppbv). Values that we assume to be too high are marked as open circles in Fig. 2. The highest values measured in this section (11.4 kyr BP, 404 ppbv; 16.3 kyr BP, 297 ppbv) are out of range and are marked by arrows at the corresponding time. The long lifetime of N_2O excludes variations of 20 ppbv or more in only a few years. Therefore, the high values cannot represent the atmospheric N_2O concentration and are probably due to an artefact (*18*).

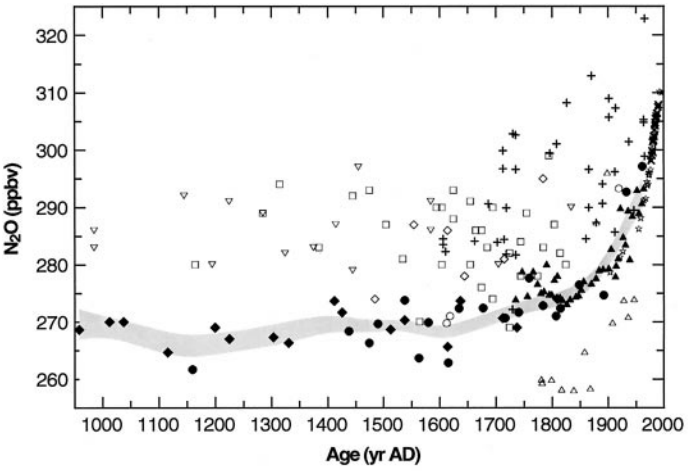

Fig. 1. Comparison of our N_2O measurements with previously published values for the past 1000 years. Shown are EUROCORE (●) and GRIP mean values (◆) from this study and the calculated 1σ band of EUROCORE and GRIP mean values (shaded area). Previously published data are from Law-dome (+) (*3*), Byrd (▽), Crête (◇), Camp Century (□) (*4*), D57 (○) (*5*), Dye 3 (△) (*6*), H15 (▲) (*7*), the South Pole (☆) (*15*), and direct atmospheric measurements from Cape Grim (×) (*14*). Each point of our record is either a single measurement or the mean value of two to six measurements on samples from the same core section. The error bars represent the analytical reproducibility (1σ). For the age scale, the difference between the age of the air and of the surrounding ice has been taken into account (*20*). The 1σ band through our data was obtained by a Monte Carlo simulation (*25*) and marks the range of a likely evolution of the N_2O concentration for this period.

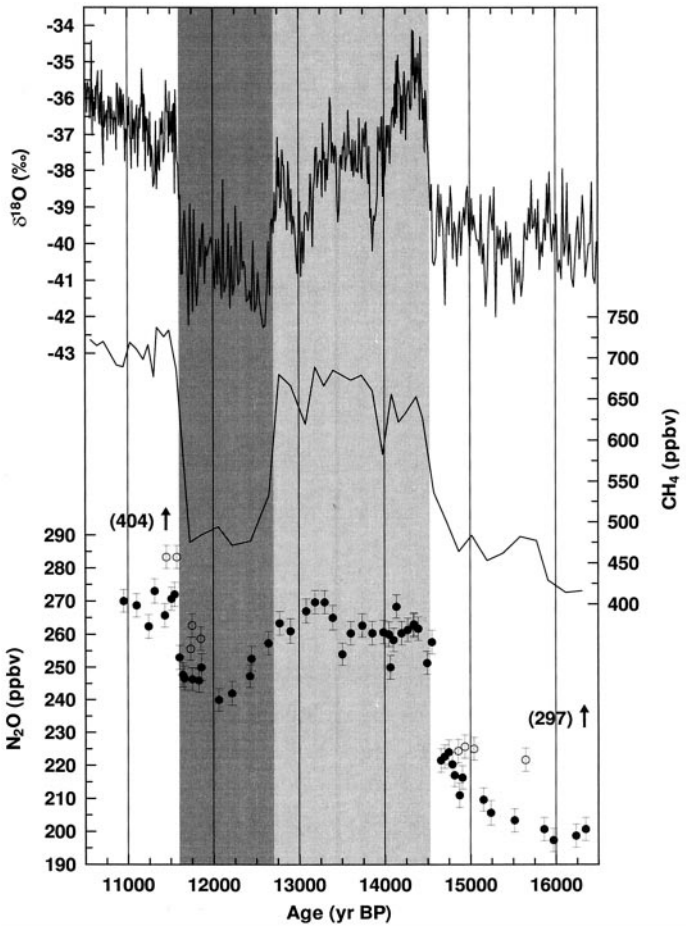

Fig. 2. GRIP N_2O (solid and open circles), $\delta^{18}O$ (*16*) (upper trace), and CH_4 (*17*) (lower trace) records for the last glacial-interglacial transition [the GRIP time scale is in years before 1989 (*20*, *26*)]. For N_2O, the results from all individual samples are plotted together with their analytical uncertainty (1σ). We assume that high N_2O values (open circles) are caused by artefacts. Solid circles indicate reliable results. Error bars indicate estimated 1σ uncertainty (4 ppbv). Measurements that are out of range are marked by arrows at the corresponding time. The light shading denotes the time period of the B/A; the dark shading denotes the YD event. The uncertainty in the difference between ice and gas ages (Δage) and therefore in the comparison of N_2O and CH_4 to $\delta^{18}O$ is about 100 years (*17*).

The question arises whether the synchronous evolution of the N_2O record with the records of $\delta^{18}O$ and CH_4 could be an artefact caused by variations of the impurities in the ice with climate changes. Calcium (Ca^{++}) is a proxy for impurities in the ice and shows variations that are parallel to climatic changes. The GRIP Ca^{++} concentrations are elevated (*19*) and the N_2O values are depleted during the YD event. However, there is a clear depth shift for the beginning as well as for the termination of the two signals in the ice core. Such a shift is expected if the measured N_2O signal corresponds to the atmospheric concentration, because of the age difference between ice and enclosed air (*20*). If reactions with chemical impurities caused the N_2O signal, no such shift would be expected. We conclude that it is very unlikely that the whole N_2O record during fast climate changes is an artefact caused by chemical impurities in the ice.

In the GRIP record covering a fast climate oscillation during the last ice age—Dansgaard-Oeschger (D-O) event 8 (36.5 to 33.5 kyr BP)—the N_2O concentration increased from below 210 ppbv to over 250 ppbv and decreased again to less than 210 ppbv within 3.5 kyr (Fig. 3). The highest value measured in this time period (302 ppbv at 36.0 kyr BP) is marked by an arrow at the corresponding time in Fig. 3. For the same time period, 13 samples of the Byrd ice core from Antarctica (80°S, 120°W) were analyzed as well (Fig. 3). Given today's small interhemispheric gradient of approximately 1 ppbv (*1*), we expect that the interhemispheric difference was also small during D-O event 8 and that therefore the measurements from the two cores should be almost the same within the analytical uncertainty. The Byrd measurements indicate an increase in the N_2O concentration from approximately 210 ppbv to a maximum value of 247 ppbv around 35 kyr BP. The increase at the beginning of D-O event 8 and the absolute values during the mild phase are in good agreement with our GRIP results. This agreement between two records from ice cores that differ significantly in their chemical impurities strongly supports our assumption that the general N_2O record measured in Greenland ice represents the atmospheric concentration.

The general pattern of N_2O variations is similar to that for CH_4, with lower concentrations during cold climate stages and higher concentrations during warm ones. Like CH_4, N_2O seems to be coupled with Greenland temperature and therefore to the climate

changes in the Northern Hemisphere, whereas the temperature reconstructed for Antarctica shows a different pattern (*17*). The preindustrial emission rate of the natural sources is estimated at 11×10^{12} g of nitrogen per year (11 Tg of N year^{-1}) (*21*). We assume for the following estimates that the lifetime of N_2O was constant and therefore that the equilibrium concentration was proportional to the annual emission rates. Lower concentrations in the past suggest that emission rates assuming equilibrium states were reduced by 10% (1.1 Tg of N year^{-1}) during the YD event and by about 26% (2.9 Tg of N year^{-1}) in the late glacial relative to preindustrial emission rates. During D-O event 8, the concentration changed by about 50 ppbv, corresponding to an emission rate change of 2 Tg of N year^{-1}. These are significant changes in any single natural source. Additional information about environmental changes in response to climatic changes is expected from measurements of changes in the interhemispheric gradient of N_2O and of time lags between changes in the concentrations of CH_4 and N_2O. The interhemispheric gradient cannot be determined with the present precision of measurements. Time lags are especially pronounced during the two transitions from mild events with a relatively high N_2O concentration to cold events with a low N_2O concentration. The decreases of N_2O at the end of the warmer epochs started at the same time or even before the decreases of CH_4 and the final decrease of $\delta^{18}O$ after a last peak value, but occurred more slowly. Only part of the delayed decrease of N_2O as compared to CH_4 after a climate cooling can be attributed to the longer atmospheric lifetime of the former.

At the end of D-O event 8, the CH_4 concentration showed its highest value at about 34.5 kyr BP (Fig. 3) and decreased over about 500 years to a value typical for the cold phases. Assuming a linear decrease of the N_2O source from 10.4 to 8.4 Tg of N year^{-1} in the same time period as the CH_4 sources, we would expect a N_2O concentration below 210 ppbv at about 33.8 kyr BP (*22*). Therefore, we conclude that the reduction of N_2O sources was slower than that of methane sources at the end of D-O event 8.

The difference is even more pronounced at the transition from the Bølling/Allerød (B/A) (14.5 to 12.7 kyr BP) to the YD (12.7 to 11.6 kyr BP) (Fig. 3). The CH_4 concentration decreased very quickly, indicating a reduction of methane sources to late glacial levels within 250 years or less. If N_2O sources had been reduced in the same time span to late glacial levels, we would expect a concentration of about 200 ppbv in the middle of the YD period despite the longer lifetime of N_2O. The N_2O sources were reduced more slowly than the CH_4 sources and, in contrast to CH_4 sources, did not reach a usual cold phase level (about 8 Tg of N year^{-1}) during the YD event.

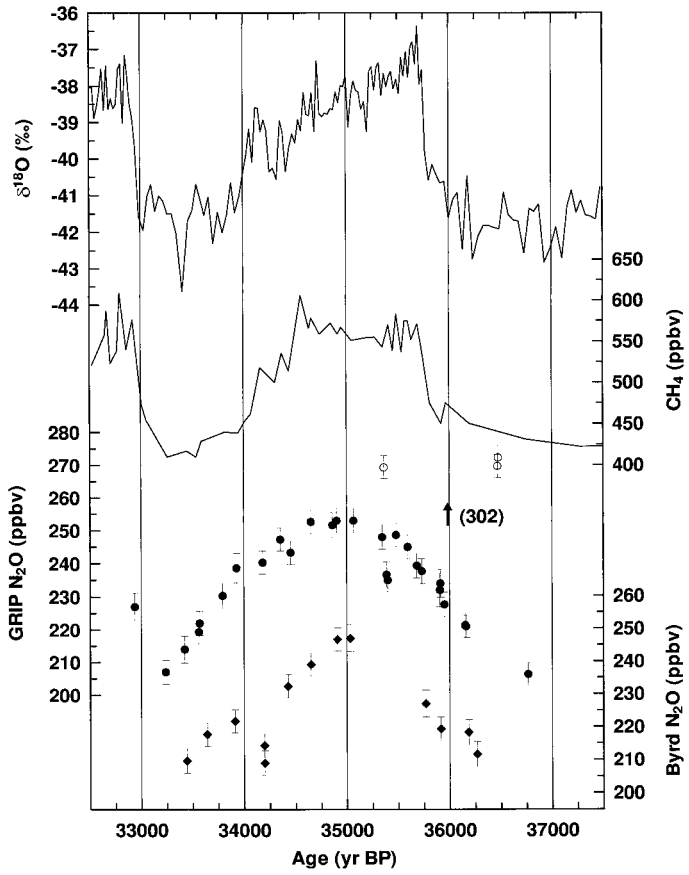

Fig. 3. GRIP N_2O (solid circles, left axis), $\delta^{18}O$ (*16*) (upper trace), and CH_4 (*17*) (lower trace) records for D-O event 8. We assume that high N_2O values (open circles and arrow at the corresponding time) are caused by an artefact. For this time period, the uncertainty in Δage is better than 300 years (*17*). N_2O measurements from the Byrd core for the same time period are shown as solid diamonds (right axis). Error bars indicate estimated 1σ uncertainty (4 ppbv). The time scale of the Byrd gas record was synchronized to that of the GRIP gas record with an uncertainty of 200 years (*17*).

Time lags during increases of the N_2O concentration at the beginning of mild phases or of the Holocene are less obvious. The increase at the beginning of D-O event 8 is difficult to determine because there is a gap of results between 36.2 and 36.7 kyr BP. An increase in the N_2O concentration of 50 ppbv occurred either in 1250 years or in a little less than 1000 years. However, the increase in the source was a gradual one. The increases at the beginning of the B/A and the Holocene are difficult to determine because of results that we consider to be affected by artefacts. N_2O started to increase slowly at about 16 kyr BP to reach a level of about 220 ppbv in 14.8 kyr BP and was followed by a fast increase of about 45 ppbv in 300 years. At the YD-to-Holocene transition, the N_2O concentration increased by 30 ppbv in about 200 years. Considering the present uncertainty, the increases at the beginning of the B/A and the Holocene can either be explained by an immediate increase of the sources or a gradual increase within 300 and 200 years, respectively, as shown by very simple model calculations.

The main candidates for changing sources of N_2O are the oceans and terrestrial soils. The N_2O production in soils depends mainly on the input of organic matter, fertility, moisture status, temperature, and oxygen status (*23*). The oceanic N_2O source depends not only on N_2O production but also on the transport of N_2O from depth (*24*) to the surface water. Climate changes influence both sources, but their individual contribution and even the sign of their response to climate variations are difficult to estimate. Because both oceanic and terrestrial sources can change very quickly, even the rate of a N_2O increase (for example, from the last glacial to the B/A) is not sufficient to constrain the sources. On the basis of our data, we cannot yet determine the sources responsible for the N_2O concentration changes discussed here.

An identification of sources will only become possible when the isotopic signature of N_2O trapped in ice can be measured accurately. However, it is not a priori clear whether N_2O trapped in ice keeps its isotopic signature over centuries and millennia. Comparison of additional high-resolution N_2O records with CH_4 (mainly terrestrial source) and CO_2 records (largely influenced by the oceanic source) and identification of leads and lags of concentration changes of these three greenhouse gases during climate changes will provide more detailed information about the response of the environment to climate changes. In addition, model simulations of oceanic and terrestrial sources should be performed to further constrain the N_2O source history on the basis of measurements of past N_2O changes.

References and Notes

1. M. Prather *et al.*, in *Climate Change 1994*, J. T. Houghton *et al.*, Eds. (Cambridge Univ. Press, New York, 1995), pp. 73–126.
2. This data is from the National Oceanic and Atmospheric Administration/Climate Monitoring and Diagnostics Laboratory air sampling network (available at www.cmdl.noaa.gov/ftpdata.html).
3. D. M. Etheridge, G. I. Pearman, F. de Silva, *Ann. Glaciol.* **10**, 28 (1988).
4. M. A. K. Khalil and R. A. Rasmussen, *ibid.*, p. 73.
5. D. Zardini *et al.*, *J. Atmos. Chem.* **8**, 189 (1989).
6. M. Leuenberger and U. Siegenthaler, *Nature* **360**, 449 (1992).
7. T. Machida *et al.*, *Geophys. Res. Lett.* **22**, 2921 (1995).
8. J. Chappellaz *et al.*, *Nature* **366**, 443 (1993).
9. T. Blunier *et al.*, *ibid.* **374**, 46 (1995).
10. J. Chappellaz *et al.*, *J. Geophys. Res.* **102**, 15987 (1997).
11. For the N_2O measurements the refreezing temperature was held at –25°C.
12. The extraction causes a loss of $(2.32 \pm 0.47) \times 10^{-8}$ ml of N_2O (at standard temperature and pressure), corresponding to a concentration correction of about 6 ppbv with a typical sample size of 40 g of ice.
13. The enrichment due to gravitational fractionation is 1.5 ppbv for the GRIP samples from the past millennium and 1.7 to 2.3 ppbv for the other GRIP samples. The Byrd samples have to be corrected by 1.0 to 1.1 ppbv. The results presented here have not been corrected.
14. R. G. Prinn *et al.*, in *Trends '93: A Compendium of Data on Global Change*, T. A. Boden, D. P. Kaiser, R. J. Sepanski, F. W. Stoss, Eds. (ORNL/CDIAC-65) (Carbon Dioxide Information Analysis Center, Oak Ridge National Laboratory, Oak Ridge, TN, 1994), pp. 396–420.
15. M. Battle *et al.*, *Nature* **383**, 231 (1996).
16. W. Dansgaard *et al.*, *ibid.* **364**, 218 (1993).
17. T. Blunier *et al.*, *ibid.* **394**, 739 (1998).
18. A surplus of N_2O could be caused by a chemical reaction in the ice, as in the case of CO_2 [M. Anklin, J.-M. Barnola, J. Schwander, B. Stauffer, D. Raynaud, *Tellus* **47 B**, 461 (1995); H. J. Smith, M. Wahlen, D. Mastroianni, K. Taylor, P. Mayewski, *J. Geophys. Res.* **102**, 26577 (1997)] and CO [D. Haan and D. Raynaud, *ibid.* **50B**, 253 (1998)]; a postcoring effect (for example, because of the infiltration of bore hole liquid into micro cracks); or an analytical artefact. We remeasured a sample from the same depth range, 0.07 m deeper in the core than that with the highest N_2O concentration, and again obtained about the same value (410 and 397 ppbv, respectively). This test rules out an accidental error or contamination during extraction and analysis, but it does not rule out the possibility that N_2O could be produced during the extraction in the melt water because of chemical impurities or a postcoring effect. We observed that the artefacts are very local in the ice core; a third measurement 0.51 m deeper in the core than the highest result showed a value of 283 ppbv. The same effect was observed in four other cases. At present, we cannot identify any reactions that would produce N_2O in the meltwater or in the ice.
19. K. Fuhrer *et al.*, *Atmos. Environ.* **27A**, 1873 (1993).
20. J. Schwander *et al.*, *J. Geophys. Res.* **102**, 19483 (1997).
21. C. Kroeze, A. Moiser, L. Bouwman, *Global Biogeochem. Cycles* **13**, 1 (1999).
22. The calculations were made with a one-box atmospheric model [M. A. K. Khalil and R. A. Rasmussen, *Ann. Glaciol.* **10**, 73 (1988)].
23. A. F. Bouwman *et al.*, *Global Biogeochem. Cycles* **7**, 557 (1993).
24. J. E. Dore *et al.*, *Nature* **396**, 63 (1998).
25. For the Monte Carlo simulation, 1000 runs were simulated. Each run takes into account the fact that the deviations from the mean values show a Gaussian distribution and calculates a smoothed spline with a cutoff period of 300 years [I. G. Enting, *J. Geophys. Res.* **92**, 10977 (1987)]. The 1σ band is given by the mean and the standard deviation of all splines.
26. S. J. Johnsen *et al.*, *Nature* **359**, 311 (1992).
27. This work, as part of GRIP, was supported by the University of Bern, the Swiss National Science Foundation, the European Community program "Environment and Climate 1994–1998," the Fondation de France, and the Programme National d'Étude de la Dynamique de Climat. Special thanks to J. Schwander, F. Joos, and R. Knutti for fruitful conversations and to E. Wolff and two anonymous reviewers for constructive comments.

5 February 1999; accepted 4 June 1999

Optical Vortices Crystals: Spontaneous Generation in Nonlinear Semiconductor Microcavities

J. Scheuer and M. Orenstein

Broad-area, vertical-cavity surface-emitting lasers were shown to switch their emission mode from the regular single or multilobed light fields to exhibit complex arrays of "dark beams." Examination of these dark spot arrays revealed that they consist of multiple, closely packed optical vortices: optical fields that have phase singularities and show increased complexity as the injection current level is raised. Contrary to their complex appearance, most of these light distributions are not the result of a multimode (multiple-frequency) operation but exhibit single-frequency characteristics. The dark beam patterns can be described as emanating from a spontaneous process of transverse mode locking of nearly degenerate modes, assisted by the laser nonlinearity. Surprisingly, these patterns show high resemblance to patterns generated in other nonlinear scenarios that are completely different both in scale and in mechanism.

The formation and propagation of complex, transverse, spatiotemporal field patterns (dynamically evolving optical field patterns, manifested as a complex structure of high- and low-intensity areas across the optical beam) in nonlinear optical devices is both of a fundamental interest and could have applications in a variety of areas such as optical data storage, distribution and processing [exploiting the robustness of a vortex field (*1*)], and laser cooling [optical trapping of particles in the featured intensity distribution (*2*)]. The generation of global field patterns was explored recently in optical cavities incorporating a nonlinear medium (*3*–*6*). These studies focused mainly on externally driven cavities and exhibited the formation of ordered patterns of bright or dark spots with hexagonal symmetry. Other patterns, such as rolls (repeated elongated field distributions), had been observed as well (*3*). The experimental observation of these phenomena is intricate because of the requirement for high values of both the Fresnel number and the nonlinearity. As a result, "optical crystals" were observed mainly in hybrid electro-optical systems [systems that mimic a performance of an optical structure by replacing some of its more difficult-to-achieve intrinsic mechanisms (such as nonlinearity and feedback) with an electronic realization] and also in a nonlinear macrocavity containing sodium vapor (*7*).

Semiconductor microcavities under lasing condition are potentially the best microlabortories for producing and using complex optical fields because of the reasons detailed here. These devices combine a very high-quality optical cavity and a nonlinear medium. The semiconductor laser nonlinearity is of a saturation type and is unique in having an appreciable contribution from both the real and imaginary nonlinear index of refraction. The intrinsic gain of the laser assists in overcoming the losses that are a dominant factor in the deterioration of the nonlinear propagation. The vertical cavity configuration plays a major role in the pattern formation discussed

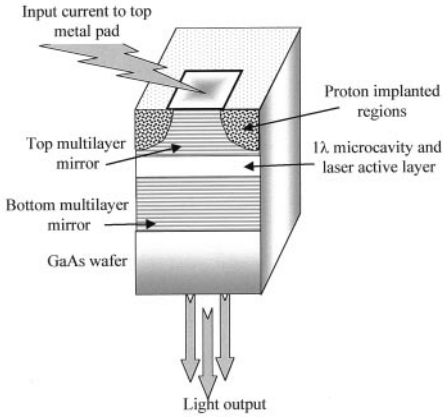

Fig. 1. Schematics of the nonlinear microcavity cross section.

Department of Electrical Engineering, Technion, Haifa 32000, Israel.